



- 1 **Title:** Sensitivity of potential evapotranspiration to changes in climate variables for different climatic zones
- 2 **Author names and affiliations:** Danlu Guo<sup>a</sup>; Seth Westra<sup>a</sup>; Holger R. Maier<sup>a</sup>.
- 3 <sup>a</sup> School of Civil, Environmental and Mining Engineering, the University of Adelaide, North Terrace, Adelaide SA
- 4 5000, Australia.
- 5 **Corresponding author:** Danlu.Guo@Adelaide.edu.au
- 6 **Permanent address:** School of Civil, Environmental and Mining Engineering, the University of Adelaide, North
- 7 Terrace, Adelaide SA 5000, Australia.



8 **Abstract**

9 Understanding the factors that impact on the sensitivity of potential evapotranspiration (PET) to changes in  
10 different climate variables is critical to assessing the possible implications of anthropogenic climate change on  
11 the catchment water balance. Using global sensitivity analysis, this study assessed the implications of baseline  
12 climate conditions on the sensitivity of PET to a large range of plausible changes in temperature ( $T$ ), relative  
13 humidity ( $RH$ ), solar radiation ( $R_s$ ) and wind speed ( $u_z$ ). The analysis was conducted at 30 Australian locations  
14 representing different climatic zones, using the Penman-Monteith and Priestley-Taylor PET models. Results from  
15 both models suggest that the baseline climate can have a substantial impact on overall PET sensitivity. In  
16 particular, approximately 2-fold greater changes in PET were observed in cool-climate energy-limited locations  
17 compared to other locations in Australia, indicating the potential for elevated water loss as a result of increasing  
18 actual evapotranspiration (AET) in these locations. The two PET models consistently indicated temperature to  
19 be the most important variable for PET, but showed large differences in the relative importance of the  
20 remaining climate variables. In particular, for the Penman-Monteith model wind and relative humidity were the  
21 second-most important variable for dry and humid catchments, respectively, whereas for the Priestley-Taylor  
22 model solar radiation was the second-most important variable, particularly for warmer catchments. This  
23 information can be useful to inform the selection of suitable PET models to estimate future PET for different  
24 climate conditions, providing evidence on both the structural plausibility and input uncertainty for the  
25 alternative models.

26 **Keywords:** climate impact assessment; evapotranspiration; Penman-Monteith; climate zones; Priestley-Taylor;  
27 global sensitivity analysis

28



## 29 1. Introduction

30 Evapotranspiration (ET) is critical in assessing the impacts of anthropogenic climate change on the catchment  
31 water balance, with ET fluxes accounting for about 62% of land-surface precipitation on average globally  
32 (Dingman, 2015) and thus representing the dominant loss of water from a large proportion of catchments  
33 worldwide. ET fluxes are affected by climate change through a cascade of processes that begins with the  
34 increasing concentration of greenhouse gases, as well as their attendant impacts on large-scale circulation and  
35 associated changes to the global distribution of energy and moisture. These large-scale processes lead to local-  
36 scale changes in the atmosphere, which in turn influence the catchment water balance through a set of  
37 terrestrial hydrological processes by which precipitation is converted into actual ET (AET), runoff and  
38 groundwater recharge (Oudin et al., 2005).

39 Climate impact studies that investigate the influence of climate forcings on the catchment water balance are  
40 usually based on projections of future climate represented by climate variables such as temperature and solar  
41 radiation from general circulation models (GCMs), which are converted into potential ET (PET) using one or  
42 several PET models. The PET projections are combined with GCM projections of precipitation (P), which  
43 together can be used to directly estimate the water deficit (Chang et al., 2016; Taylor et al., 2013). Alternatively,  
44 rainfall-runoff models can be used to translate the changes in P and PET into changes in runoff (e.g. Akhtar et  
45 al., 2008; Chiew et al., 2009; Koedyk and Kingston, 2016), as well as associated information such as the impact  
46 on catchment yield (Wilby et al., 2006), water supply security (Paton et al., 2014, 2013) and flood risk (Bell et al.,  
47 2016). Therefore, to quantify the specific impact of changes in ET on the water balance, a good understanding  
48 of the sensitivity of PET to potential changes in its key influencing climatic variables is required (e.g. Goyal,  
49 2004; Tabari and Hosseinzadeh Talaee, 2014). This is particularly relevant given the recent focus on “scenario-



50 neutral” (or “bottom-up”) approaches to climate impact assessment (Brown et al., 2012; Culley et al., 2016;  
51 Prudhomme et al., 2010), which require the sensitivity of a given system to potential changes in climate forcings  
52 to be estimated (Guo et al., 2016a; Kay et al., 2014; Prudhomme et al., 2013a; Prudhomme et al., 2013b;  
53 Steinschneider and Brown, 2013).

54 Furthermore, the sensitivity of PET can provide critical evidence in relation to which models are most  
55 appropriate for PET estimation under climate change conditions, which is particularly relevant to the ongoing  
56 debate on the potential trade-off between model complexity and reliability. Complex models such as the  
57 Penman-Monteith model are often recommended for their ability to represent the physical processes that  
58 affect PET (Barella-Ortiz et al., 2013; Donohue et al., 2010; McVicar et al., 2012), such as potential compensating  
59 effects between temperature and wind that may explain the paradox that decreasing pan evaporation (which is  
60 closely related to PET) has been observed with increasing temperatures for many locations worldwide (McVicar  
61 et al., 2008; Roderick et al., 2007). However, simpler empirical models may be preferable under some  
62 conditions, as they require a smaller number of input climate variables, which might be able to be projected  
63 with greater confidence with GCMs (Ekström et al., 2007; Kay and Davies, 2008). For example, there is  
64 reasonable confidence in projections of temperature and relative humidity in Australia for a given emission  
65 scenario, but less confidence in projections of wind due to sub-grid effects of orography and other land-surface  
66 features (CSIRO and Bureau of Meteorology, 2015; Flato et al., 2013). In these situations, models such as the  
67 Priestly-Taylor model that do not depend on wind may produce more reliable estimates of PET compared to the  
68 more complex Penman-Monteith model. Thus, the choice of climate variables to include in climate impact  
69 assessments must be informed both by the relative importance of each variable on projections of PET (e.g.



70 Tabari and Hosseinzadeh Talaei, 2014), and the likely confidence in projections of each variable (e.g. Flato et  
71 al., 2013; Johnson and Sharma, 2009).

72 Sensitivity analysis methods have been employed in a number of recent studies to assess the overall sensitivity  
73 of PET to potential changes in climate, as well as to better understand the relative importance of different  
74 climate variables on overall PET sensitivity. For example, Goyal (2004) found that PET was most sensitive to  
75 perturbations in temperature, followed by solar radiation, wind speed and vapor pressure, at a single study site  
76 in an arid region in India. Tabari and Hosseinzadeh Talaei (2014) also looked at the sensitivity of PET to  
77 perturbations of historical climate data from eight meteorological stations representing four climate types in  
78 Iran, and concluded that the importance of wind speed and air temperature was lower while that of sunshine  
79 hours was higher for a humid location compared to an arid location. Gong et al. (2006) found that the  
80 differences in PET sensitivity across the upper, middle and lower regions of the Changjiang (Yangtze) basin in  
81 China are largely due to contrasting baseline wind speed patterns. However, most of these PET sensitivity  
82 analysis studies focused on a limited number of study sites and/or climatic zones, so that the specific causes for  
83 varying PET sensitivity at different locations, such as the roles of climatic and hydrological conditions, remain  
84 unclear. Consequently, it is difficult to extrapolate our existing knowledge of PET sensitivity and the relative  
85 importance of each atmospheric variable to new locations, which is essential for assessing the water balance at  
86 regional scales.

87 To address the shortcomings of existing studies outlined above, this study aims to gain an understanding of (i)  
88 the sensitivity of PET estimates to changes in the key climatic variables which influence PET, and how these  
89 sensitivity estimates are affected by baseline hydrologic and climatic conditions; and (ii) the relative importance  
90 of these climatic variables for PET, and how this changes with the baseline hydrologic and climatic conditions.



91 These aims were achieved by analyzing the sensitivity of PET to perturbations in four of its driving climatic  
92 variables, namely temperature ( $T$ ), relative humidity ( $RH$ ), solar radiation ( $R_s$ ) and wind speed ( $u_2$ ), at 30 study  
93 sites across Australia representing a range of climate zones. Both the Penman-Monteith and Priestly-Taylor  
94 models were used, as they represent different conceptualizations of the PET process and also have been widely  
95 used for climate impact assessments (Arnell, 1999; Donohue et al., 2009; Felix et al., 2013; Gosling et al., 2011;  
96 Kay et al., 2009; Prudhomme and Williamson, 2013). Since the impact of climate-induced changes in one  
97 climate variable can be amplified or offset by changes in another variable (for examples see Lu et al., 2016;  
98 Roderick and Farquhar, 2002; Su et al., 2015), a global sensitivity analysis method was used, with similar  
99 methods being successfully applied to account for the impact of joint variations in the input variables on the  
100 output of a range of environmental models (e.g. Guillevic et al., 2002; Nossent et al., 2011; Tang et al., 2007a;  
101 van Griensven et al., 2006). The results were presented in terms of both absolute and relative sensitivity scores,  
102 and presented to elucidate the specific roles of the baseline hydro-climatic condition on the PET sensitivity.

103 The subsequent sections of this paper are structured as follows. Section 2 introduces the data obtained from  
104 the 30 study sites required for the global sensitivity analysis. Section 3 describes the approach to the global  
105 sensitivity analysis of PET. Section 4 presents and discusses two sets of results to assess (i) the estimated PET  
106 sensitivity to potential changes in temperature, solar radiation, humidity and wind; and (ii) the relative  
107 importance of the four climate variables for estimating PET, for each PET model. The study is summarized and  
108 concluded in Sect. 5.



## 109 2. Data

110 To represent contrasting hydro-climatic conditions for assessing PET sensitivity, we selected case study  
111 locations within different Köppen classes in Australia. The original Köppen climate classification (Köppen et al.,  
112 1930; Köppen, 1931) provides a useful categorization of hydro-climatic conditions at specific locations, which is  
113 based on the long-term average levels and seasonal patterns of climatic and hydrologic variables, including  
114 temperature, relative humidity and rainfall. The classification system has been later adapted for Australia,  
115 referred to as the “modified Köppen classification” (as in Stern et al., 2000) and is now widely used in climatic  
116 and hydrologic studies to categorize case study locations (e.g. Johnson and Sharma, 2009; Li et al., 2014;  
117 Rustomji et al., 2009).

118 As mentioned in the Introduction, both the Penman-Monteith and the Priestley-Taylor models were used to  
119 estimate PET for the global sensitivity analysis. The estimation of PET with these models relies on temperature,  
120 relative humidity, solar radiation and (for the Penman-Monteith model only) wind speed. In addition, the  
121 rainfall data were also obtained to assess the aridity of the different locations. We limited the selection of study  
122 sites to those with 10 or more years of continuous climate data with no more than 5 % missing records over the  
123 study period. This led to a final selection of 30 weather stations (Fig. 1), with a consistent data period from 1  
124 January 1995 to 31 December 2004. The data obtained at each site are detailed as below:

- 125 • **Daily maximum and minimum temperature ( $T$  in °C), maximum and minimum relative humidity ( $RH$   
126 **in %) and wind speed ( $u_z$  in  $m s^{-1}$ ):** Data for each of these variables were obtained directly from each  
127 weather station.**



- 128 • **Daily solar radiation ( $R_s$  in  $\text{MJ m}^{-2} \text{day}^{-1}$ ):** Daily solar radiation was calculated from daily sunshine hour  
129 data ( $n$  in h) obtained from each weather station, using the Ångström-PreScott equation as in McMahon  
130 et al. (2013).
- 131 • **Daily rainfall (mm):** Daily rainfall data were obtained from a rain gauge at each weather station.

132 **Figure 1: Locations of 30 Australian weather stations (see Table 1 for the full names of these weather stations)**  
133 **selected for analysis, with reference to their corresponding climate classes derived following the modified Köppen**  
134 **classification (reproduced with data from Stern et al., 2000).**  
135

136 Table 1 shows the average levels of the four ET-related climate variables, as well as the rainfall within the study  
137 period, at each of the 30 sites. As can be seen, there are large differences in the average values of each variable,  
138 highlighting large differences in the climatic conditions across the 30 sites. In addition, a quantity particularly  
139 relevant to ET processes is the long-term averaged ratio of PET to precipitation (PET/P), which describes  
140 whether a location is water-limited (PET/P >1) or energy-limited (PET/P < 1). This ratio was also estimated for  
141 each site and is shown in Table 1 (with the point colour in Fig. 1 indicating whether the location is water-limited  
142 or energy-limited). The range of PET/P values indicates substantial variations in the water availability conditions  
143 at different study sites. Note that these ratios were based on the estimates of PET from the Penman-Monteith  
144 model, which generally suggested similar PET/P ratios to those estimated from Priestly-Taylor.

145 **Table 1: Names, locations and average climate conditions of the 30 weather stations over the study period (1995-**  
146 **2004).**  
147





## 148 3. Method

### 149 3.1. Overview

150 A schematic of the approach followed in study is shown in Fig. 2. As a required model input for the global  
151 sensitivity analysis, a large number of representative samples were first obtained for the four climate variables  
152 which influence PET ( $T$ ,  $RH$ ,  $R_s$  and  $u_2$ ) at each study site, by perturbing the corresponding historical climate data  
153 (Sect. 3.2). The outputs of the global sensitivity analysis (i.e. the responses of PET) were estimated with the  
154 Penman-Monteith and Priestley-Taylor models (Sect. 3.3). Using the perturbations of climate variables and the  
155 responses of PET, a global sensitivity analysis was conducted (Sect. 3.4), with the analysis divided into two parts:

- 156 (1) To assess the sensitivity of PET, the percentage changes in PET in response to all the climate  
157 perturbations were estimated relative to the baseline PET at each location. To generalize the results,  
158 the sensitivity obtained from each PET model was also plotted against the baseline levels of each  
159 climate variable for all study sites.
- 160 (2) To assess the relative importance of each climate variable, the PET sensitivity to all climate  
161 perturbations in (1) was first compared to the conditional sensitivity when holding each variable  
162 constant. This comparison enables an assessment of the relative impact of each variable on the total  
163 PET sensitivity. An alternative presentation of the individual and interaction effects of the climate  
164 variables was achieved using the Sobol' method (Sobol' et al., 2007), in which the total variance of PET  
165 was estimated based on different samples drawn from the perturbed ranges of each climate variable,  
166 and was then partitioned the into the individual contribution from each climate variable and their  
167 interactions (see Appendix A.1. for details). The Sobol' first-order sensitivity indices were estimated and



168 plotted against the baseline levels of each climate variable for all study sites to explore the role of  
169 baseline climate on the relative importance of each climatic variable for PET.

170 **Figure 2: Schematic of the method used in this study.**

172 3.2. Representing plausible changes in the climatic variables

173 As part of the global sensitivity analysis, a large number of representative combinations of the changes in the  
174 four climate variables considered ( $T$ ,  $RH$ ,  $R_s$  and  $u_z$ ) were obtained. The upper and lower bounds for perturbing  
175 each climate variable were determined based on the uncertainty bounds of projections for 2100 for Australia  
176 (Stocker et al., 2013). The selected bounds are given in Table 2, which are all slightly wider than those presented  
177 in Stocker et al. (2013) to encompass a comprehensive range of plausible future climate change scenarios.  
178 Within these bounds, samples were drawn for different combinations of changes in each climatic variable. Latin  
179 hypercube sampling (LHS) was used for this purpose due to its effectiveness in covering multi-dimensional input  
180 spaces (Osidele and Beck, 2001; Sieber and Uhlenbrook, 2005; Tang et al., 2007b).

181 **Table 2: Plausible perturbation bounds for each climate variable relative to their current levels.**

183 In accordance with the method suggested by Nossent et al. (2011), the sample size was selected to ensure the  
184 convergence of the first- and total-order Sobol' sensitivity indices, which occurs when the width of the 95 %  
185 confidence intervals from 1000-fold bootstrap resampling of the each index is below 10 % of the corresponding  
186 mean obtained from bootstrapping. Specifically, we generated different sizes of LHS samples of climate  
187 perturbations with the historical climate data from one study site, from which the PET responses were  
188 estimated using the Penman-Monteith model. The 1000-fold bootstrap estimates for the Sobol' first- and total-



189 order sensitivity indices for each climate variable were then derived (as in Eqn. 2 and 5 in Appendix A.1.,  
190 respectively) for each sample size. It was observed that both the Sobol' indices began to converge when the  
191 sample size exceeded 5000, which was therefore used as the LHS sample size for all the sensitivity experiments  
192 in this study.

193 The 5000 joint perturbations to the four climate variables obtained by LHS were treated as change factors and  
194 applied to the time series of daily values of the corresponding historical data in order to generate 5000 time  
195 series of climate affected daily data. Rather than using a single daily mean value of temperature and relative  
196 humidity, the two PET models used in this study require both the daily minimum and maximum values;  
197 therefore each pair of temperature variables and relative humidity variables was considered jointly and thus  
198 perturbed by the same amount for each day.

### 199 3.3. Estimating PET responses to climate perturbation

200 To represent the responses in PET as a result of the climate perturbations, we used both the Penman-Monteith  
201 and Priestley-Taylor models, which provide contrasting process representations to estimate PET. The Penman-  
202 Monteith model is often referred to as a combinational model, as it combines the energy balance and mass  
203 transfer components of ET, and takes into account vegetation-dependent processes such as aerodynamic and  
204 surface resistances. The model requires input of six climate variables, namely,  $T_{\max}$ ,  $T_{\min}$ ,  $RH_{\max}$ ,  $RH_{\min}$ ,  $R_s$  and  $u_z$ .  
205 The Priestley-Taylor model consists of a simpler structure, considering only the energy balance, without  
206 consideration of mass transfer or any impact from vegetation. Therefore, the Priestley-Taylor model is also  
207 referred to as a radiation-based model. The model only requires five climate variables, including  $T_{\max}$ ,  $T_{\min}$ ,  
208  $RH_{\max}$ ,  $RH_{\min}$  and  $R_s$ .



209 To minimize the potential confounding effects of differences in vegetated surface, the evaporative surface was  
210 assumed to be reference crop for all study sites, so that it was possible to use the FAO-56 version of the  
211 Penman-Monteith model (Allen et al., 1998). The detailed formulations of the two PET models, as well as use of  
212 constants and assumptions are included in McMahon et al. (2013). Both models were implemented using the R  
213 package *Evapotranspiration* (<http://cran.r-project.org/web/packages/Evapotranspiration/index.html>) (Guo et  
214 al., 2016b). From each model, two sets of estimated PET were obtained: (i) a single set of baseline (historical)  
215 PET data at each study site with the historical climate data; (ii) 5000 sets of perturbed PET data at each study  
216 site corresponding to the 5000 sets of perturbed climate data obtained using LHS, as detailed in Sect. 3.2.

### 217 3.4. Analyses of PET sensitivity

218 To assess the overall sensitivity of PET to plausible climate change, we first estimated the percentage changes in  
219 PET (relative to the baseline PET) using all climate perturbations at the 30 study sites, with estimates from both  
220 the Penmen-Monteith and Priestley-Taylor models. A closer investigation of how PET sensitivity varies with  
221 baseline climate was conducted by plotting all PET responses against the average levels of each climate variable,  
222 for all study sites and all months. The reason for the choice of monthly timescale is that for some study sites,  
223 the climate can vary substantially by season, so that an annual analysis might obscure important sub-annual  
224 effects.

225 To assess the relative importance of each climate variable for PET estimation from each model, we first  
226 compared two sets of PET sensitivity, including:

- 227 (1) The unconditional sensitivity of PET obtained from the entire 5000 sets of climate perturbations from  
228 LHS;



229 (2) The conditional sensitivity of PET on no-change in each climatic variable, obtained using a subset of all  
230 climate perturbations used in (1), for which the changes in the specific conditioning climatic variable  
231 were close to zero (within  $\pm 0.1$  °C for  $T$ , and within  $\pm 0.1$  % for the other three variables).

232 In this way any difference between (1) and (2) was purely contributed by the impact of changing the specific  
233 conditioning climate variable. To quantify and compare the relative importance of each climate variable, we  
234 then utilized the Sobol' method, which was implemented within the R package *sensitivity* ([https://cran.r-](https://cran.r-project.org/web/packages/sensitivity/index.html)  
235 [project.org/web/packages/sensitivity/index.html](https://cran.r-project.org/web/packages/sensitivity/index.html)). We estimated the Sobol' first-order sensitivity indices (as in  
236 Eqn. 2, Appendix A.1.) to assess the role of each individual climate variable for each PET model, at the 30 study  
237 sites. The sum of all interaction effects was also calculated for each location as the difference between the sum  
238 of all first-order indices and one (Eqn. 6, Appendix A.1.). The Sobol' first-order indices were then plotted against  
239 the baseline levels of each climate variable at the 30 study sites, to assess how the relative importance changes  
240 with the baseline climatic conditions.

## 241 4. Results and discussion

### 242 4.1. Sensitivity of PET to potential climate change for different climate zones

243 We start by assessing the sensitivity of PET to the full set of climate perturbations at the 30 study sites at the  
244 annual timescale, using both the Penman-Monteith and Priestley-Taylor models. The sensitivity results are  
245 presented in Table 3 in terms of the minimum, maximum and average changes of PET relative to the 1995-2004  
246 baseline based on the 5000 LHS replicates at each study site. The two models suggest similar average PET  
247 sensitivity at most locations, with the sensitivity of the Penman-Monteith model averaged across all the  
248 locations (+13.38 %) being slightly higher than that for the Priestley-Taylor model (+10.91 %). Greater



249 differences between the two models were observed when considering the ranges of sensitivity values. In  
250 particular, the minimum and maximum values (averaged across all the 30 sites) were -13.66 % and +47.09 % for  
251 the Penman-Monteith model, respectively, compared to -7.39 % and +34.47 % for the Priestley-Taylor model.  
252 This corresponds to a range for the Penman-Monteith model being approximately 45 % wider than that of the  
253 Priestley-Taylor model.

254 **Table 3: Annual average PET sensitivity to the full set of climate perturbations (as % changes to baseline PET) from**  
255 **the Penman-Monteith and Priestley-Taylor models at the 30 study sites relative to the 1995-2004 baseline. The**  
256 **maximum and minimum sensitivity values from each model are shaded in grey.**  
257

258 For each PET model, the sensitivity values display substantial variation across the locations, with both models  
259 suggesting the lowest PET sensitivity at arid locations and highest PET sensitivities at humid locations, as was  
260 also observed in Tabari and Hosseinzadeh Talaei (2014). Specifically, the Penman-Monteith model identified  
261 the highest average PET sensitivity at Flinders Island (+17.15 %), with the lowest sensitivity at Alice Springs  
262 (+9.80 %). The Priestley-Taylor model identified the highest average PET sensitivity at Hobart (+17.77 %), with  
263 the lowest at Tennant Creek (+7.09 %).

264 To further investigate how PET sensitivity varies with different climatic conditions, we now focus on the  
265 associations between the PET sensitivity and the baseline levels of the four climate variables for each month of  
266 the year and across the 30 study sites. Starting with the Penman-Monteith model (Fig. 3), it is clear that the PET  
267 sensitivity displays clear association with the baseline levels of climate variables, with higher sensitivity values  
268 for locations that are cooler (low  $T$ ), more humid (high  $RH$ ), and receiving less solar radiation (low  $R_s$ ). The  
269 highest associations can be found with  $T$  (Fig. 3a), with the monthly changes in PET ranging from -30.2% to  
270 +98.3 % for the lowest baseline  $T$  value of 5.0 °C, compared to a range of -13.3 % to +46.6 % for the highest



271 baseline  $T$  of 30.3 °C. Similarly, the range of Penman-Monteith PET sensitivity values also shows clear decreases  
272 with baseline  $R_s$  (Fig. 3c), and increases with baseline  $RH$  (Fig. 3b). The baseline  $u_z$  (Fig. 3d) levels show no  
273 obvious impact on the PET sensitivity.

274 **Figure 3: Monthly PET responses from the Penman-Monteith model, plotted against the monthly baseline levels of (a)**  
275 **temperature, (b) relative humidity, (c) solar radiation and (d) wind speed at 30 study sites. Each interval represents**  
276 **the range of all PET responses to the full set of climate perturbations for a single month at a single location, with the**  
277 **mean represented by the point on the line. The classification of energy- and water-limited months are based on the**  
278 **corresponding monthly PET/P ratios.**

279

280 The sensitivity from Priestley-Taylor was also investigated (Fig. 4), and results are consistent with the results  
281 from the Penman-Monteith model, although the overall ranges were lower for each variable as anticipated  
282 from the results in Table 3. Interestingly, regardless of the choice of PET model, the range of sensitivity values at  
283 the monthly scale is higher than the range for the annual scale suggesting greater uncertainty at higher  
284 temporal resolutions.

285 **Figure 4: Monthly PET responses from the Priestley-Taylor model, plotted against the monthly baseline levels of (a)**  
286 **temperature, (b) relative humidity, (c) solar radiation and (d) wind speed at 30 study sites. Each interval represents**  
287 **the range of all PET responses to the full set of climate perturbations for a single month at a single location, with the**  
288 **mean represented by the point on the line. The classification of energy- and water-limited months are based on the**  
289 **corresponding monthly PET/P ratios.**

290

291 In addition to impact of baseline climatic conditions, we are also interested in the role of baseline hydrological  
292 conditions (represented by the PET/P ratio at each study site, calculated on a monthly basis as hydrological  
293 conditions can vary substantially over the course of a year) on PET sensitivity. These results are also shown in  
294 Fig. 3 and 4, with red-colored bars denoting water-limited conditions, and blue-colored bars denoting energy-  
295 limited conditions. These figures show that PET sensitivity is generally larger under energy-limited conditions,



296 regardless of the choice of PET model. In contrast, for water-limited conditions, most sensitivity magnitudes  
297 only vary within approximately half of the entire range from each PET model. However, when exploring the  
298 association with temperature (Fig. 3a and 4a) in more detail, the sensitivity is in fact lowest for energy-limited  
299 conditions during warm months (i.e. as when  $T > 25$  °C, corresponding to the monsoonal summer months in the  
300 northern parts of Australia), and highest for the energy-limited conditions during cool months (i.e. as when  $T <$   
301  $15$  °C, corresponding to the wet winter months in southern Australia). This highlights that it is the atmospheric  
302 temperature, rather than the level of aridity, that appears to affect the overall sensitivity. This finding lead to a  
303 different interpretation to previous studies, which indicated that the dominant drivers of spatially varying PET  
304 include aridity (Tabari and Hosseinzadeh Talaei, 2014) and wind speed (Gong et al., 2006).

305 The above results also have potential implications on likely AET changes in a future climate. In particular, the  
306 above analysis shows that cool and humid regions and seasons appear to show the greatest sensitivity to PET,  
307 and given that water is not expected to be limited for these cases, the ratio between AET and PET is also likely  
308 to be the greatest for these cases. As such, one might expect a greater change to AET occurring at the locations  
309 and times of the year where PET is most sensitive to changes in climate.

310 As a potential limitation to the above analysis, reliability issues of the Penman-Monteith model discussed in a  
311 recent study (Milly and Dunne, 2016) suggest that the Penman-Monteith model may overestimate the  
312 sensitivity in these energy-limited regions relative to a GCM-based AET benchmark. They concluded that the  
313 potential changes in ET would be better described by GCMs than “off-line” PET models (such as the two models  
314 used in this study), as GCMs can explicitly consider more complex atmospheric processes, such as the  
315 interaction between  $\text{CO}_2$  and stomatal conductance. Nevertheless, it should be noted that the current reliability  
316 of GCMs in simulating ET is also questionable, due to the uncertainty in representing soil moisture and radiative





317 energy at the evaporative surface (e.g. Barella-Ortiz et al., 2013; Boé and Terray, 2008; Seneviratne et al., 2013).  
318 In addition, due to the coarse scale of GCM output, downscaling is generally required to post-process output for  
319 use at local and regional scales, which often adds further bias and uncertainties to the GCM simulation and  
320 largely limits their applicability (e.g. Chen et al., 2012; Diaz-Nieto and Wilby, 2005). Therefore, although GCM  
321 results may be more suitable for large-scale assessments, catchment-scale climate impact assessments are  
322 likely to be informed by “off-line” PET models for the foreseeable future. Consequently, the sensitivity results  
323 shown in this study are likely to remain relevant for climate impact assessments conducted using these models.

#### 324 4.2. Relative importance of climate variables affecting PET for different climate zones

325 We now explore the relative importance of each climate variable on overall PET sensitivity, by first visualizing  
326 the conditional sensitivity of PET when holding each variable constant at its historical level while perturbing the  
327 remaining variables, and comparing this to the unconditional sensitivity estimates (as shown in Fig. 3 and Fig. 4).  
328 Figure 5 shows the ranges of the monthly unconditional PET sensitivity (dashed lines) and the PET sensitivity  
329 conditioned on zero-change in each of  $T$ ,  $RH$ ,  $R_s$  and  $u_z$  (solid lines) for the Penman-Monteith model, plotted  
330 against the monthly baseline levels of the four climate variables at the 30 study sites.

331 **Figure 5: Monthly PET responses from the Penman-Monteith model, plotted against the monthly baseline levels of (a)**  
332 **temperature, (b) relative humidity, (c) solar radiation and (d) wind speed at 30 study sites. Each dashed (solid) line**  
333 **represents the range of all PET responses to the full set of climate perturbations (conditioned on no-change in each**  
334 **climate variable) for a single month at a single location. The corresponding means are represented by the points on**  
335 **the lines. The classification of energy- and water-limited months are based on the corresponding monthly PET/P**  
336 **ratios.**

337

338 The figure suggests that perturbations in  $T$  have the greatest impact on PET sensitivity compared to other  
339 climate variables (Fig. 5a), contributing to at least 45 % of the PET responses compared to the unconditional



340 results. Humidity also plays a significant role, although only for higher humidity levels (contributing up to 57 %  
341 of PET responses) with relatively minor influence for the less humid catchments (Fig. 5b). In contrast, the role of  
342 solar radiation (Fig. 5c) and wind (Fig. 5d) is generally minor, with the unconditional sensitivities being only  
343 slightly wider than the conditional sensitivities.

344 A similar analysis was conducted for the Priestley-Taylor model (Fig. 6), and shows somewhat different results  
345 compared to those obtained for the Penman-Monteith model. Consistent with Fig. 5a, temperature has the  
346 greatest impact, but in this case contributes up to 85 % of the overall variability (Fig. 6a). As a result, the  
347 sensitivity values for the remaining variables are correspondingly much lower. Unlike in Fig. 5b, the role of  
348 relative humidity does not appear to increase significantly with increasing baseline humidity (Fig. 6b) and in  
349 general contributes less than 33 % of the overall variability. The role of solar radiation appears to be somewhat  
350 larger for high baseline solar radiation values (Fig. 6c) and wind is shown to have no impact as expected, since  
351 wind is not an input into the Priestley-Taylor model (Fig. 6d) However, it is worth noting that although the  
352 Priestley-Taylor model does not consider wind as an input variable, the unconditional sensitivity is slightly wider  
353 than the sensitivity conditioned on no-change in wind. This is because the conditional sensitivity is estimated  
354 with only a subset of all climate perturbations (Sect. 3.4), which may not consist of the entire range of  
355 perturbation in each of the other three climate variables.

356 **Figure 6: Monthly PET responses from the Priestley-Taylor model, plotted against the monthly baseline levels of (a)**  
357 **temperature, (b) relative humidity, (c) solar radiation and (d) wind speed at 30 study sites. Each dashed (solid) line**  
358 **represents the range of all PET responses to the full set of climate perturbations (conditioned on no-change in each**  
359 **climate variable) for a single month at a single location. The corresponding means are represented by the points on**  
360 **the lines. The classification of energy- and water-limited months are based on the corresponding monthly PET/P**  
361 **ratios.**

362



363 A more formal quantitative measure of the relative importance of each climate variable for PET is provided by the  
364 Sobol' indices. The Sobol' first-order indices of PET to changes in the four climate variables at the annual scale,  
365 as well as their interactions, are presented in Fig. 7 for the Penman-Monteith model, which are plotted against  
366 the baseline levels of each climatic variable. For presentation purposes, the baseline levels are represented by  
367 the rank of the baseline annual average value of each variable, rather than the absolute level of each climate  
368 variable across the 30 study sites. The Sobol' indices in the figure show that  $T$  is generally the most important  
369 variable for PET, with index values ranging from 0.46 to 0.62. Since the Sobol' indices suggest the partitioning of  
370 the total variance in PET, these results are consistent with Fig. 5a, which suggests that perturbations in  $T$   
371 contribute to at least 45 % of the variation in the estimated changes in PET. The role of wind and humidity in  
372 affecting the sensitivity values is also evident, with wind being the second-most important variable (with Sobol'  
373 indices up to 0.42) for sites with low baseline humidity, and humidity being the second-most important variable  
374 (with Sobol' indices up to 0.47) for sites that have high humidity (Fig. 7b). Solar radiation is generally the  
375 variable with the lowest Sobol' indices, although the largest contributions (up to 18 %) can be observed for  
376 warm catchments (Fig. 7a).

377 **Figure 7: Sobol' first-order sensitivity indices of the Penman-Monteith model for changes in the four climate**  
378 **variables (colored) and their interaction effects (grey), plotted against the ranking of the average level of each climate**  
379 **variable at 30 study sites**

380

381 The Sobol' sensitivity indices are also presented for the Priestley-Taylor model (Fig. 8), and show substantial  
382 differences compared to those for the Penman-Monteith model. Temperature exhibits the largest sensitivity  
383 score in most cases, and ranges from 0.44 to 0.83. The relative role of temperature varies most clearly as a  
384 function of both the baseline temperature (Fig. 8a) and the baseline solar radiation values (Fig. 8c), with



385 temperature being particularly important for low temperature and low solar radiation sites. As temperature and  
386 radiation increase, the relative role of solar radiation becomes more important, reaching Sobol' index values of  
387 up to 0.49. In contrast, the role of relative humidity is generally minor (with Sobol' indices within the range  
388 0.03-0.1) and does not appear to vary as a function of baseline conditions. Finally, the role of wind is absent,  
389 given that this variable is not included as part of the Priestley-Taylor equation.

390 **Figure 8: Sobol' first-order sensitivity indices of the Priestley-Taylor model for changes in the four climate variables**  
391 **(colored) and their interaction effects (grey), plotted against the ranking of the average level of each climate variable**  
392 **at 30 study sites**  
393

394 The differences between the Penman-Monteith and Priestley-Taylor models highlight the different physical  
395 assumptions underpinning the models, with aerodynamic processes being important for the Penman-Monteith  
396 model as indicated by the relative importance of  $RH$  and  $u_z$  for this model, whereas  $R_s$  has a critical role in the  
397 Priestley-Taylor model, which is closely linked to the emphasis of radiative energy as the energy source for ET in  
398 the model.

399 Finally, comparing Fig. 7 and Fig. 8, it is apparent that the interactions among the four climate variables on PET  
400 (shown as grey bars) are greater in the Penman-Monteith model compared to the Priestley-Taylor model.  
401 Specifically, these interactions contribute to 0.03-0.04, and 0-0.02 of the total variance in PET for the Penman-  
402 Monteith and Priestley-Taylor models, respectively. The relative magnitude of the interaction effects in the two  
403 models can be again related to their structural differences: the higher interaction effects in Penman-Monteith  
404 can be a result of the larger number of variables in this model compared with those in the Priestley-Taylor  
405 model.



406 It is difficult to assess the consistency of these sensitivity results with existing literature, given the different  
407 methodologies and datasets used in other studies. Although most PET sensitivity studies used only the Penman-  
408 Monteith PET model there is still substantial discrepancy in results depending on the specific implementations  
409 of sensitivity analysis. For example, Gong et al. (2006) perturbed each of temperature, wind speed, relative  
410 humidity and solar radiation within  $\pm 20\%$  for the Changjiang basin in China, and observed that that relative  
411 humidity was generally the most important variable driving PET, followed by solar radiation, temperature and  
412 wind speed. This contrasted with our results from the Penman-Monteith model, which showed temperature as  
413 the most important variable and solar radiation as the least important variable for almost all the stations  
414 analyzed, and may be attributable to the different baseline climates as well as the ranges used for the sensitivity  
415 analysis between the two studies.

416 The results of our study were more consistent with Goyal (2004), who concluded that PET is most sensitive to  
417 potential changes in temperature for an arid region in India, by applying a  $\pm 20\%$  perturbation on each of  
418 temperature, solar radiation, wind speed and vapor pressure. In contrast, Tabari and Hosseinzadeh Talaei  
419 (2014) also used a  $\pm 20\%$  perturbation range, but on only three climate variables, including temperature, wind  
420 speed and sunshine hours for several climate regions in Iran. Their study concluded that the catchment aridity  
421 was a major determinant of the sensitivity to temperature, wind speed and humidity, whereas our analysis  
422 highlights the importance of baseline temperature and humidity, rather than the aridity (or water- or energy-  
423 limited status of the catchment) as a key driver.

424 PET sensitivity can be further diversified by the choice of PET models, as illustrated in McKenney and Rosenberg  
425 (1993), in which the percentage changes in PET due to a  $+6\text{ }^\circ\text{C}$  change can differ up to around  $40\%$ , when  
426 estimated with eight alternative PET models. This lack of consistency in the relative importance of the climate



427 variables for PET is not surprising given the findings of our study, as the results are strongly dependent on the  
428 design of the sensitivity analysis experiment, including the choice of study sites and study periods, the input  
429 climate variables considered, and the ways to perturb them (i.e. the choice of global or local perturbation and  
430 the ranges of perturbation in different input variables).

431 Nevertheless, the sensitivity results from this study suggest some distinct spatial patterns of the relative  
432 importance of different climate variables in Australia. Since the Penman-Monteith model is the most  
433 comprehensive physically-based PET model, the above regionalization of the PET sensitivity from this model can  
434 be used as a benchmark to identify the key climate variables for estimating PET under potential climate change.  
435 This information can be particularly useful to suggest the potential suitability of specific PET models for regional  
436 applications. For example, since the Penman-Monteith PET showed higher sensitivity to wind at dry locations  
437 (Fig. 7b), it is expected that wind-dependent PET models (such as Penman and Penman-Monteith) would be  
438 more appropriate for predicting PET at these locations; in contrast, using simpler models that do not consider  
439 wind as an input (such as Priestley-Taylor) can be problematic for these locations. Although this study only  
440 examined two PET models, the results suggest that simpler empirical models are likely to ignore some potential  
441 dynamics and interactions within the climate variables, which makes them less preferred for PET estimation  
442 under changing climates.

443 Another particular issue in the selection of one or several PET models under a changing climate arises from  
444 considering the current reliability of available climate projections, as the models can show high levels of  
445 sensitivity to variables for which we currently do not have high-quality climate projections. For example, for a  
446 given emissions scenario, there is reasonable confidence in projections of temperature and relative humidity in  
447 Australia, but less confidence in projections of solar radiation and wind (CSIRO and Bureau of Meteorology,



448 2015; Flato et al., 2013). However the radiation-based Priestley-Taylor model can show high sensitivity to solar  
449 radiation, particularly for warm locations with high baseline solar radiation (Fig. 8a and 8c), due to a particular  
450 emphasis on radiative energy and thus the empirical relationships between PET and solar radiation. Similarly,  
451 the Penman-Monteith model can exhibit higher sensitivity to wind for locations with low relative humidity (Fig.  
452 7b). Therefore, the use of GCM projections at these locations may lead to significant uncertainty in PET  
453 estimates due to the uncertainty in the driving variables.

## 454 5. Summary and conclusions

455 In this study, we used a global sensitivity analysis to investigate the sensitivity of PET and the relative  
456 importance four climatic variable which influence PET ( $T$ ,  $RH$ ,  $R_s$  and  $u_z$ ) under plausible changes in these  
457 variables. The sensitivity analysis was conducted at 30 Australian case study locations with contrasting hydro-  
458 climatic conditions for generalization of the results. For the sensitivity analysis, the historical climate data at  
459 each study site were first perturbed to represent a large number of plausible climate change conditions, and  
460 then the responses in PET were estimated with both the Penman-Monteith and Priestley-Taylor models, from  
461 which the sensitivity of PET was analyzed. The key results were as follows:

- 462 • In general PET is most sensitive to potential changes in climate in regions with lower temperature, less  
463 solar radiation and greater humidity, where 2-fold greater changes in PET are expected compared to  
464 other locations in Australia.
- 465 • Within the plausible perturbations in  $T$ ,  $RH$ ,  $R_s$  and  $u_z$ , PET is generally most sensitive to  $T$ . The relative  
466 importance of the other climate variables varies substantially with the PET models.  $R_s$  has a dominant  
467 role in the radiation-based Priestley-Taylor model, highlighting the importance of radiative energy in



468 the model. In contrast, the importance of  $RH$  and  $u_z$  are comparable for the Penman-Monteith model,  
469 whereas  $R_s$  has only little impact, reflecting the contribution of aerodynamic energy.

- 470 • The relative importance of climate variables in influencing PET depends very clearly on baseline climatic  
471 conditions. From Penman-Monteith, locations that are warmer, drier and receiving more solar radiation  
472 generally show greater sensitivity to  $u_z$  and lower sensitivity to  $RH$ . For Priestley-Taylor, the importance  
473 of  $T$  increases while that of  $R_s$  decreases for cooler locations and locations receiving less solar radiation.

474 The global sensitivity analysis used in this study is a powerful tool for providing a comprehensive and consistent  
475 measure of PET sensitivity to different climatic variables, considering a wide range of possible changes in  
476 climate, across different models with different data requirements. However, we have identified space for  
477 improvements in further implementations. For example, the bounds of perturbation for each climate variable  
478 can have a substantial impact on PET sensitivity, and thus their selection requires careful justification (for  
479 example see Shin et al., 2013; Whateley et al., 2014). Therefore, alternative lines of evidence on possible  
480 changes in climate should be considered in setting these bounds: for example, the results of ensemble climate  
481 models (e.g. Collins et al., 2013), the impact of low-frequency climatic modes (e.g. Chen et al., 2013; Vincent et  
482 al., 2015), as well as findings from within paleoclimatology records (e.g. Ault et al., 2014; Ho et al., 2015).

483 The analysis in this study also lends itself to scenario-neutral analyses (Brown et al., 2012; Prudhomme et al.,  
484 2010), although the full implications on specific impacts of hydrological systems (e.g. flood risk, water supply,  
485 etc) would require the sensitivity analysis to be propagated to runoff via explicitly modelling the interaction  
486 between ET and rainfall-runoff processes (e.g. Garcia and Tague, 2015; Roy et al., 2016). Furthermore, potential  
487 changes to precipitation, which were not analyzed here but which can have a significant impact on future  
488 runoff, would need to be considered. Within this context, the incorporation of alternative lines of evidence can





489 therefore not only be used to define the bounds of the perturbations, but can also be superimposed onto the  
490 exposure space (e.g. as in Culley et al., 2016; Prudhomme et al., 2013a) to provide insight into the likelihood of  
491 possible changes. The outcomes of our study can feed into such a scenario-neutral analysis by providing  
492 guidance on the variables that are likely to be most important for a particular location, as well as providing  
493 insights on the potential implications of using alternative PET models on the overall sensitivity results.

## 494 References

- 495 Akhtar, M., Ahmad, N., and Booij, M. J.: The impact of climate change on the water resources of Hindukush–  
496 Karakorum–Himalaya region under different glacier coverage scenarios, *Journal of Hydrology*, 355, 148-163,  
497 2008.
- 498 Allen, R. G., Pereira, L. S., Raes, D., and Smith, M.: Crop evapotranspiration-Guidelines for computing crop water  
499 requirements-FAO Irrigation and drainage paper 56, FAO, Rome, 300, 6541, 1998.
- 500 Arnell, N. W.: The effect of climate change on hydrological regimes in Europe: a continental perspective, *Global*  
501 *Environmental Change*, 9, 5-23, 1999.
- 502 Ault, T. R., Cole, J. E., Overpeck, J. T., Pederson, G. T., and Meko, D. M.: Assessing the Risk of Persistent Drought  
503 Using Climate Model Simulations and Paleoclimate Data, *Journal of Climate*, 27, 7529-7549, 2014.
- 504 Barella-Ortiz, A., Polcher, J., Tuzet, A., and Laval, K.: Potential evaporation estimation through an unstressed  
505 surface-energy balance and its sensitivity to climate change, *Hydrol. Earth Syst. Sci.*, 17, 4625-4639, 2013.
- 506 Bell, V. A., Kay, A. L., Davies, H. N., and Jones, R. G.: An assessment of the possible impacts of climate change on  
507 snow and peak river flows across Britain, *Climatic Change*, 136, 539-553, 2016.
- 508 Boé, J. and Terray, L.: Uncertainties in summer evapotranspiration changes over Europe and implications for  
509 regional climate change, *Geophysical Research Letters*, 35, n/a-n/a, 2008.
- 510 Brown, C., Ghile, Y., Laverty, M., and Li, K.: Decision scaling: Linking bottom-up vulnerability analysis with  
511 climate projections in the water sector, *Water Resources Research*, 48, W09537, 2012.
- 512 Chang, S., Graham, W. D., Hwang, S., and Muñoz-Carpena, R.: Sensitivity of future continental United States  
513 water deficit projections to general circulation models, the evapotranspiration estimation method, and the  
514 greenhouse gas emission scenario, *Hydrol. Earth Syst. Sci.*, 20, 3245-3261, 2016.
- 515 Chen, H., Xu, C.-Y., and Guo, S.: Comparison and evaluation of multiple GCMs, statistical downscaling and  
516 hydrological models in the study of climate change impacts on runoff, *Journal of Hydrology*, 434–435, 36-45,  
517 2012.
- 518 Chen, W., Lan, X., Wang, L., and Ma, Y.: The combined effects of the ENSO and the Arctic Oscillation on the  
519 winter climate anomalies in East Asia, *Chinese Science Bulletin*, 58, 1355-1362, 2013.
- 520 Chiew, F. H. S., Teng, J., Vaze, J., Post, D. A., Perraud, J. M., Kirono, D. G. C., and Viney, N. R.: Estimating climate  
521 change impact on runoff across southeast Australia: Method, results, and implications of the modeling method,  
522 *Water Resources Research*, 45, W10414, 2009.



- 523 Collins, M., Knutti, R., Arblaster, J., Dufresne, J.-L., Fichfet, T., Friedlingstein, P., Gao, X., Gutowski, W. J., Johns,  
524 T., Krinner, G., Shongwe, M., Tebaldi, C., Weaver, A. J., and Wehner, M.: Long-term Climate Change: Projections,  
525 Commitments and Irreversibility. In: *Climate Change 2013: The Physical Science Basis. Contribution of Working  
526 Group I to the Fifth Assessment Report of the Intergovernmental Panel on Climate Change*, Stocker, T. F., Qin,  
527 D., Plattner, G.-K., Tignor, M., Allen, S. K., Boschung, J., Nauels, A., Xia, Y., Bex, V., and Midgley, P. M. (Eds.),  
528 Cambridge University Press, Cambridge, United Kingdom and New York, NY, USA, 2013.
- 529 CSIRO and Bureau of Meteorology: *Climate Change in Australia Information for Australia's Natural Resource  
530 Management Regions: Technical Report*, CSIRO and Bureau of Meteorology, Australia, 2015.
- 531 Culley, S., Noble, S., Yates, A., Timbs, M., Westra, S., Maier, H. R., Giuliani, M., and Castelletti, A.: A bottom-up  
532 approach to identifying the maximum operational adaptive capacity of water resource systems to a changing  
533 climate, *Water Resources Research*, doi: 10.1002/2015WR018253, 2016. n/a-n/a, 2016.
- 534 Diaz-Nieto, J. and Wilby, R. L.: A comparison of statistical downscaling and climate change factor methods:  
535 impacts on low flows in the River Thames, United Kingdom, *Climatic Change*, 69, 245-268, 2005.
- 536 Dingman, S. L.: *Physical Hydrology: Third Edition*, Waveland Press, 2015.
- 537 Donohue, R. J., McVicar, T. R., and Roderick, M. L.: Can dynamic vegetation information improve the accuracy of  
538 Budyko's hydrological model?, *Journal of hydrology*, 390, 23-34, 2010.
- 539 Donohue, R. J., McVicar, T. R., and Roderick, M. L.: Generating Australian potential evaporation data suitable for  
540 assessing the dynamics in evaporative demand within a changing climate, 2009. 2009.
- 541 Ekström, M., Jones, P., Fowler, H., Lenderink, G., Buishand, T., and Conway, D.: Regional climate model data  
542 used within the SWURVE project? 1: projected changes in seasonal patterns and estimation of PET, *Hydrology  
543 and Earth System Sciences Discussions*, 11, 1069-1083, 2007.
- 544 Felix, T. P., Petra, D., Stephanie, E., and Martina, F.: Impact of climate change on renewable groundwater  
545 resources: assessing the benefits of avoided greenhouse gas emissions using selected CMIP5 climate  
546 projections, *Environmental Research Letters*, 8, 024023, 2013.
- 547 Flato, G., Marotzke, J., Abiodun, B., Braconnot, P., Chou, S. C., Collins, W., Cox, P., Driouech, F., Emori, S., and  
548 Eyring, V.: Evaluation of climate models. In: *Climate Change 2013: The Physical Science Basis. Contribution of  
549 Working Group I to the Fifth Assessment Report of the Intergovernmental Panel on Climate Change*, Cambridge  
550 University Press, 2013.
- 551 Garcia, E. S. and Tague, C. L.: Subsurface storage capacity influences climate–evapotranspiration interactions in  
552 three western United States catchments, *Hydrol. Earth Syst. Sci.*, 19, 4845-4858, 2015.
- 553 Gong, L., Xu, C.-y., Chen, D., Halldin, S., and Chen, Y. D.: Sensitivity of the Penman–Monteith reference  
554 evapotranspiration to key climatic variables in the Changjiang (Yangtze River) basin, *Journal of Hydrology*, 329,  
555 620-629, 2006.
- 556 Gosling, S. N., Taylor, R. G., Arnell, N. W., and Todd, M. C.: A comparative analysis of projected impacts of  
557 climate change on river runoff from global and catchment-scale hydrological models, *Hydrol. Earth Syst. Sci.*, 15,  
558 279-294, 2011.
- 559 Goyal, R. K.: Sensitivity of evapotranspiration to global warming: a case study of arid zone of Rajasthan (India),  
560 *Agricultural Water Management*, 69, 1-11, 2004.
- 561 Guillevic, P., Koster, R. D., Suarez, M. J., Bounoua, L., Collatz, G. J., Los, S. O., and Mahanama, S. P. P.: Influence  
562 of the Interannual Variability of Vegetation on the Surface Energy Balance—A Global Sensitivity Study, *Journal  
563 of Hydrometeorology*, 3, 617-629, 2002.



- 564 Guo, D., Westra, S., and Maier, H. R.: An inverse approach to perturb historical rainfall data for scenario-neutral  
565 climate impact studies, *Journal of Hydrology*, doi: <http://dx.doi.org/10.1016/j.jhydrol.2016.03.025>, 2016a.  
566 2016a.
- 567 Guo, D., Westra, S., and Maier, H. R.: An R package for modelling actual, potential and reference  
568 evapotranspiration, *Environmental Modelling & Software*, 78, 216-224, 2016b.
- 569 Ho, M., Kiem, A. S., and Verdon-Kidd, D. C.: A paleoclimate rainfall reconstruction in the Murray-Darling Basin  
570 (MDB), Australia: 1. Evaluation of different paleoclimate archives, rainfall networks, and reconstruction  
571 techniques, *Water Resources Research*, 51, 8362-8379, 2015.
- 572 Johnson, F. and Sharma, A.: Measurement of GCM skill in predicting variables relevant for hydroclimatological  
573 assessments, *Journal of Climate*, 22, 4373-4382, 2009.
- 574 Kay, A. L., Crooks, S. M., and Reynard, N. S.: Using response surfaces to estimate impacts of climate change on  
575 flood peaks: assessment of uncertainty, *Hydrological Processes*, 28, 5273-5287, 2014.
- 576 Kay, A. L. and Davies, H. N.: Calculating potential evaporation from climate model data: A source of uncertainty  
577 for hydrological climate change impacts, *Journal of Hydrology*, 358, 221-239, 2008.
- 578 Kay, A. L., Davies, H. N., Bell, V. A., and Jones, R. G.: Comparison of uncertainty sources for climate change  
579 impacts: flood frequency in England, *Climatic Change*, 92, 41-63, 2009.
- 580 Koedyk, L. P. and Kingston, D. G.: Potential evapotranspiration method influence on climate change impacts on  
581 river flow: a mid-latitude case study, *Hydrology Research*, doi: 10.2166/nh.2016.152, 2016. 2016.
- 582 Köppen, W., Geiger, R., Borchardt, W., Wegener, K., Wagner, A., Knoch, K., Sapper, K., Ward, R. D., Brooks, C. F.,  
583 and Connor, A.: *Handbuch der klimatologie*, Gebrüder Borntraeger Berlin, Germany, 1930.
- 584 Köppen, W. P.: *Grundriss der klimakunde*, 1931. 1931.
- 585 Li, L., Maier, H. R., Partington, D., Lambert, M. F., and Simmons, C. T.: Performance assessment and  
586 improvement of recursive digital baseflow filters for catchments with different physical characteristics and  
587 hydrological inputs, *Environmental Modelling & Software*, 54, 39-52, 2014.
- 588 Lu, X., Bai, H., and Mu, X.: Explaining the evaporation paradox in Jiangxi Province of China: Spatial distribution  
589 and temporal trends in potential evapotranspiration of Jiangxi Province from 1961 to 2013, *International Soil  
590 and Water Conservation Research*, 4, 45-51, 2016.
- 591 McKenney, M. S. and Rosenberg, N. J.: Sensitivity of some potential evapotranspiration estimation methods to  
592 climate change, *Agricultural and Forest Meteorology*, 64, 81-110, 1993.
- 593 McMahon, T. A., Peel, M. C., Lowe, L., Srikanthan, R., and McVicar, T. R.: Estimating actual, potential, reference  
594 crop and pan evaporation using standard meteorological data: a pragmatic synthesis, *Hydrol. Earth Syst. Sci.*,  
595 17, 1331-1363, 2013.
- 596 McVicar, T. R., Roderick, M. L., Donohue, R. J., Li, L. T., Van Niel, T. G., Thomas, A., Grieser, J., Jhajharia, D.,  
597 Himri, Y., Mahowald, N. M., Mescherskaya, A. V., Kruger, A. C., Rehman, S., and Dinpashoh, Y.: Global review  
598 and synthesis of trends in observed terrestrial near-surface wind speeds: Implications for evaporation, *Journal  
599 of Hydrology*, 416-417, 182-205, 2012.
- 600 McVicar, T. R., Van Niel, T. G., Li, L. T., Roderick, M. L., Rayner, D. P., Ricciardulli, L., and Donohue, R. J.: Wind  
601 speed climatology and trends for Australia, 1975 – 2006: Capturing the stilling phenomenon and comparison  
602 with near - surface reanalysis output, *Geophysical Research Letters*, 35, 2008.
- 603 Milly, P. C. D. and Dunne, K. A.: Potential evapotranspiration and continental drying, *Nature Clim. Change*,  
604 advance online publication, 2016.
- 605 Nossent, J., Elsen, P., and Bauwens, W.: Sobol' sensitivity analysis of a complex environmental model,  
606 *Environmental Modelling & Software*, 26, 1515-1525, 2011.



- 607 Osidele, O. and Beck, M.: Identification of model structure for aquatic ecosystems using regionalized sensitivity  
608 analysis, *Water Science & Technology*, 43, 271-278, 2001.
- 609 Oudin, L., Hervieu, F., Michel, C., Perrin, C., Andréassian, V., Anctil, F., and Loumagne, C.: Which potential  
610 evapotranspiration input for a lumped rainfall–runoff model?: Part 2—Towards a simple and efficient potential  
611 evapotranspiration model for rainfall–runoff modelling, *Journal of Hydrology*, 303, 290-306, 2005.
- 612 Paton, F. L., Maier, H. R., and Dandy, G. C.: Including adaptation and mitigation responses to climate change in a  
613 multiobjective evolutionary algorithm framework for urban water supply systems incorporating GHG emissions,  
614 *Water Resources Research*, 50, 6285-6304, 2014.
- 615 Paton, F. L., Maier, H. R., and Dandy, G. C.: Relative magnitudes of sources of uncertainty in assessing climate  
616 change impacts on water supply security for the southern Adelaide water supply system, *Water Resources  
617 Research*, 49, 1643-1667, 2013.
- 618 Prudhomme, C., Crooks, S., Kay, A., and Reynard, N.: Climate change and river flooding: part 1 classifying the  
619 sensitivity of British catchments, *Climatic Change*, 119, 933-948, 2013a.
- 620 Prudhomme, C., Kay, A. L., Crooks, S., and Reynard, N.: Climate change and river flooding: Part 2 sensitivity  
621 characterisation for british catchments and example vulnerability assessments, *Climatic Change*, 119, 949-964,  
622 2013b.
- 623 Prudhomme, C., Wilby, R. L., Crooks, S., Kay, A. L., and Reynard, N. S.: Scenario-neutral approach to climate  
624 change impact studies: Application to flood risk, *Journal of Hydrology*, 390, 198-209, 2010.
- 625 Prudhomme, C. and Williamson, J.: Derivation of RCM-driven potential evapotranspiration for hydrological  
626 climate change impact analysis in Great Britain: a comparison of methods and associated uncertainty in future  
627 projections, *Hydrology and Earth System Sciences*, 17, 1365-1377, 2013.
- 628 Roderick, M. L. and Farquhar, G. D.: The Cause of Decreased Pan Evaporation over the Past 50 Years, *Science*,  
629 298, 1410-1411, 2002.
- 630 Roderick, M. L., Rotstayn, L. D., Farquhar, G. D., and Hobbins, M. T.: On the attribution of changing pan  
631 evaporation, *Geophysical research letters*, 34, 2007.
- 632 Roy, T., Gupta, H. V., Serrat-Capdevila, A., and Valdes, J. B.: Using Satellite-Based Evapotranspiration Estimates  
633 to Improve the Structure of a Simple Conceptual Rainfall-Runoff Model, *Hydrol. Earth Syst. Sci. Discuss.*, 2016, 1-  
634 28, 2016.
- 635 Rustomji, P., Bennett, N., and Chiew, F.: Flood variability east of Australia's great dividing range, *Journal of  
636 Hydrology*, 374, 196-208, 2009.
- 637 Saltelli, A., Annoni, P., Azzini, I., Campolongo, F., Ratto, M., and Tarantola, S.: Variance based sensitivity analysis  
638 of model output. Design and estimator for the total sensitivity index, *Computer Physics Communications*, 181,  
639 259-270, 2010.
- 640 Seneviratne, S. I., Wilhelm, M., Stanelle, T., van den Hurk, B., Hagemann, S., Berg, A., Cheruy, F., Higgins, M. E.,  
641 Meier, A., Brovkin, V., Claussen, M., Ducharne, A., Dufresne, J.-L., Findell, K. L., Ghattas, J., Lawrence, D. M.,  
642 Malyshev, S., Rummukainen, M., and Smith, B.: Impact of soil moisture-climate feedbacks on CMIP5 projections:  
643 First results from the GLACE-CMIP5 experiment, *Geophysical Research Letters*, 40, 5212-5217, 2013.
- 644 Shin, M.-J., Guillaume, J. H. A., Croke, B. F. W., and Jakeman, A. J.: Addressing ten questions about conceptual  
645 rainfall–runoff models with global sensitivity analyses in R, *Journal of Hydrology*, 503, 135-152, 2013.
- 646 Sieber, A. and Uhlenbrook, S.: Sensitivity analyses of a distributed catchment model to verify the model  
647 structure, *Journal of Hydrology*, 310, 216-235, 2005.



- 648 Sobol', I. M., Tarantola, S., Gatelli, D., Kucherenko, S. S., and Mauntz, W.: Estimating the approximation error  
649 when fixing unessential factors in global sensitivity analysis, *Reliability Engineering & System Safety*, 92, 957-  
650 960, 2007.
- 651 Steinschneider, S. and Brown, C.: A semiparametric multivariate, multi-site weather generator with low-  
652 frequency variability for use in climate risk assessments, *Water Resources Research*, doi: 10.1002/wrcr.20528,  
653 2013. n/a-n/a, 2013.
- 654 Stern, H., De Hoedt, G., and Ernst, J.: Objective classification of Australian climates, *Australian Meteorological*  
655 *Magazine*, 49, 87-96, 2000.
- 656 Stocker, T. F., Qin, D., Plattner, G.-K., Tignor, M., Allen, S. K., Boschung, J., Nauels, A., Xia, Y., Bex, V., and  
657 Midgley, P. M.: *Climate change 2013: The physical science basis*, Intergovernmental Panel on Climate Change,  
658 Working Group I Contribution to the IPCC Fifth Assessment Report (AR5)(Cambridge Univ Press, New York),  
659 2013. 2013.
- 660 Su, T., Feng, T., and Feng, G.: Evaporation variability under climate warming in five reanalyses and its association  
661 with pan evaporation over China, *Journal of Geophysical Research: Atmospheres*, 120, 8080-8098, 2015.
- 662 Tabari, H. and Hosseinzadeh Talaei, P.: Sensitivity of evapotranspiration to climatic change in different climates,  
663 *Global and Planetary Change*, 115, 16-23, 2014.
- 664 Tang, Y., Reed, P., van Werkhoven, K., and Wagener, T.: Advancing the identification and evaluation of  
665 distributed rainfall-runoff models using global sensitivity analysis, *Water Resources Research*, 43, W06415,  
666 2007a.
- 667 Tang, Y., Reed, P., Wagener, T., and Van Werkhoven, K.: Comparing sensitivity analysis methods to advance  
668 lumped watershed model identification and evaluation, *Hydrology and Earth System Sciences Discussions*, 11,  
669 793-817, 2007b.
- 670 Taylor, I. H., Burke, E., McColl, L., Falloon, P. D., Harris, G. R., and McNeall, D.: The impact of climate mitigation  
671 on projections of future drought, *Hydrol. Earth Syst. Sci.*, 17, 2339-2358, 2013.
- 672 van Griensven, A., Meixner, T., Grunwald, S., Bishop, T., Diluzio, M., and Srinivasan, R.: A global sensitivity  
673 analysis tool for the parameters of multi-variable catchment models, *Journal of Hydrology*, 324, 10-23, 2006.
- 674 Vincent, L. A., Zhang, X., Brown, R. D., Feng, Y., Mekis, E., Milewska, E. J., Wan, H., and Wang, X. L.: Observed  
675 Trends in Canada's Climate and Influence of Low-Frequency Variability Modes, *Journal of Climate*, 28, 4545-  
676 4560, 2015.
- 677 Whateley, S., Steinschneider, S., and Brown, C.: A climate change range - based method for estimating  
678 robustness for water resources supply, *Water Resources Research*, 50, 8944-8961, 2014.
- 679 Wilby, R. L., Whitehead, P. G., Wade, A. J., Butterfield, D., Davis, R. J., and Watts, G.: Integrated modelling of  
680 climate change impacts on water resources and quality in a lowland catchment: River Kennet, UK, *Journal of*  
681 *Hydrology*, 330, 204-220, 2006.
- 682 Zhang, X. Y., Trame, M. N., Lesko, L. J., and Schmidt, S.: Sobol Sensitivity Analysis: A Tool to Guide the  
683 Development and Evaluation of Systems Pharmacology Models, *CPT: Pharmacometrics & Systems*  
684 *Pharmacology*, 4, 69-79, 2015.

685

686



## 687 Appendix

### 688 A.1. Sobol sensitivity analysis (Sobol' et al., 2007)

689 Sobol' is considered as a variance-based method, in which the total variance in the output from a model is  
690 estimated with the Monte-Carlo method, using a large number of sampled perturbations in each of its input  
691 variable (Saltelli et al., 2010). The total variance is then partitioned to the contribution of each individual input  
692 variable as well as their interactions, as following (equation adapted from Zhang et al., 2015):

$$693 \quad V_Y = \sum_{i=1}^n V_i \quad + \quad \sum_{i<j} V_{ij} + \sum_{i<j<k} V_{ijk} \dots + V_{1,2,\dots,n} \quad (1)$$

694 **Individual effects** **Interactions**

695 The output from Sobol' method include (equations adapted from Nossent et al., 2011):

696 1) First-order sensitivity index, which quantifies the individual contribution of each input variable to  
697 the total variance of the model's output;

$$698 \quad S_i = \frac{V_i}{V_Y} \quad (2)$$

699 2) Second- and higher-order sensitivity index, which quantifies the contribution interactions among  
700 two or more input variables to the total variance of the model's output;

$$701 \quad \text{For second-order: } S_{ij} = \frac{V_{ij}}{V_Y} \quad (3)$$

$$702 \quad \text{For higher-order: } S_{ij\dots n} = \frac{V_{ij\dots n}}{V_Y} \quad (4)$$

703 3) Total sensitivity index, which quantifies the contribution of each input variable, including its  
704 individual effect as well as all its interactions with other input variables, to the total variance of the  
705 model's output.



706 
$$S_{Ti} = S_i + \sum_{j \neq i} S_{ij} = 1 - \frac{V_{\sim i}}{V_Y} \quad (5)$$

707 From Eqn. 1 to 4, the sum of individual effects of all input variables and all their interactions equals one  
708 (adapted from Zhang et al., 2015):

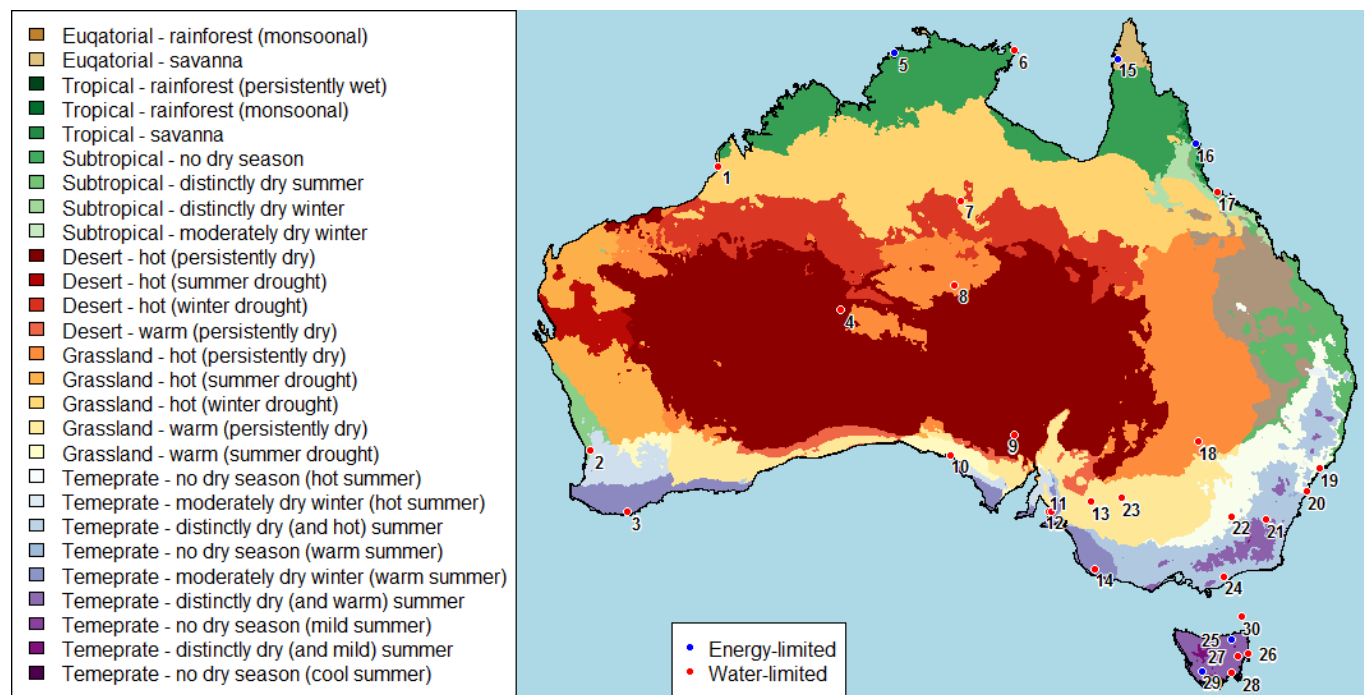
709 
$$1 = \sum_{i=1}^n S_i + \sum_{i < j} S_{ij} + \sum_{i < j < k} S_{ijk} \dots + S_{1,2,\dots,n} \quad (6)$$

710 **Individual effects**                      **Interactions**

711



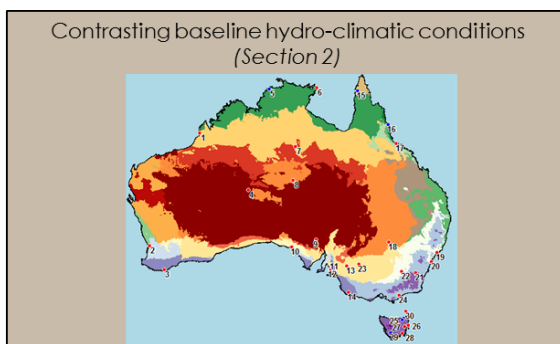
712 **Figures and Tables**



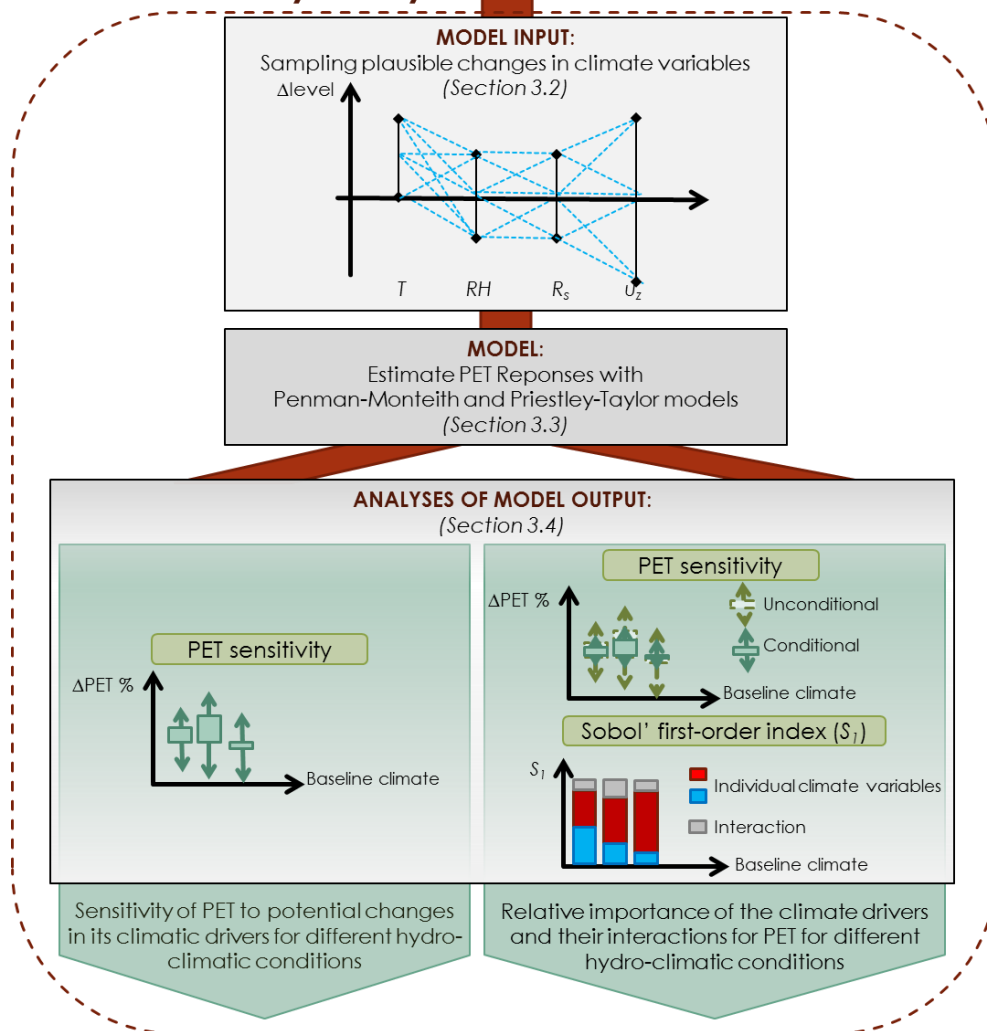
713

714 **Fig. 1e**: Locations of 30 Australian weather stations (see Table 1 for the full names of these weather stations)  
 715 selected for analysis, with reference to their corresponding climate classes derived following the modified Köppen  
 716 classification (reproduced with data from Stern et al., 2000).  
 717





## Global Sensitivity Analysis

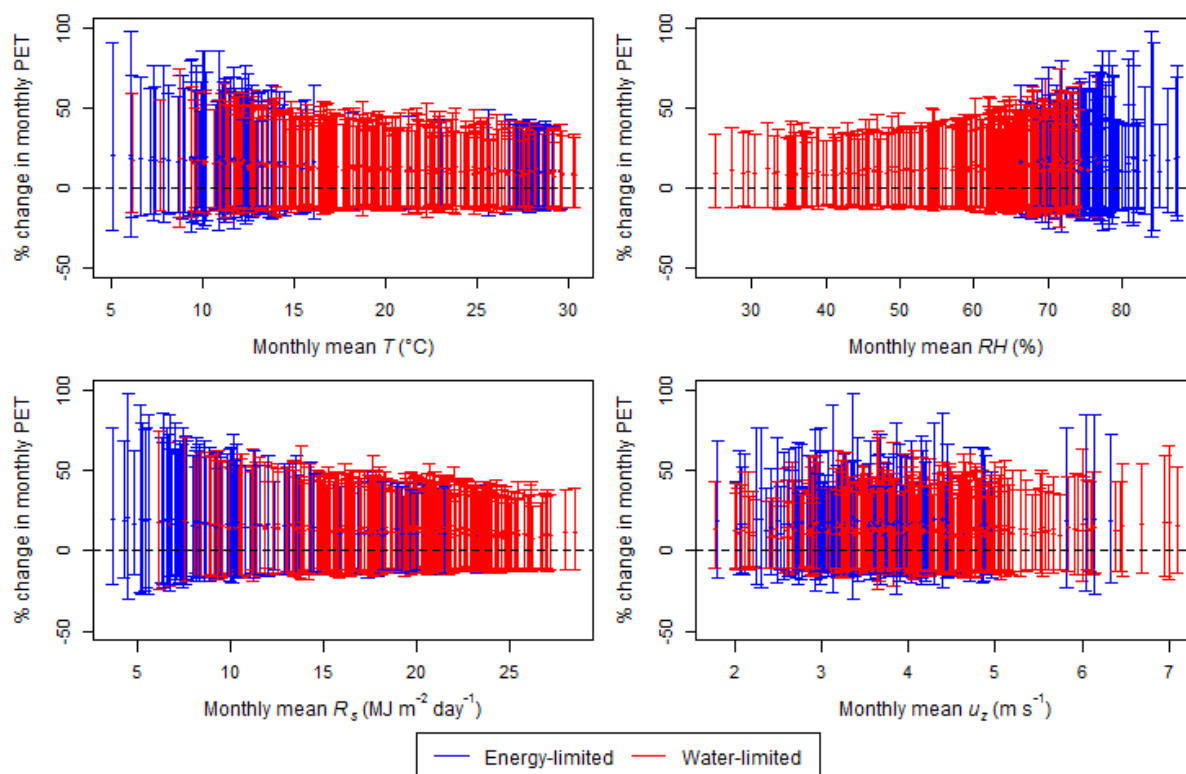


718

719

720

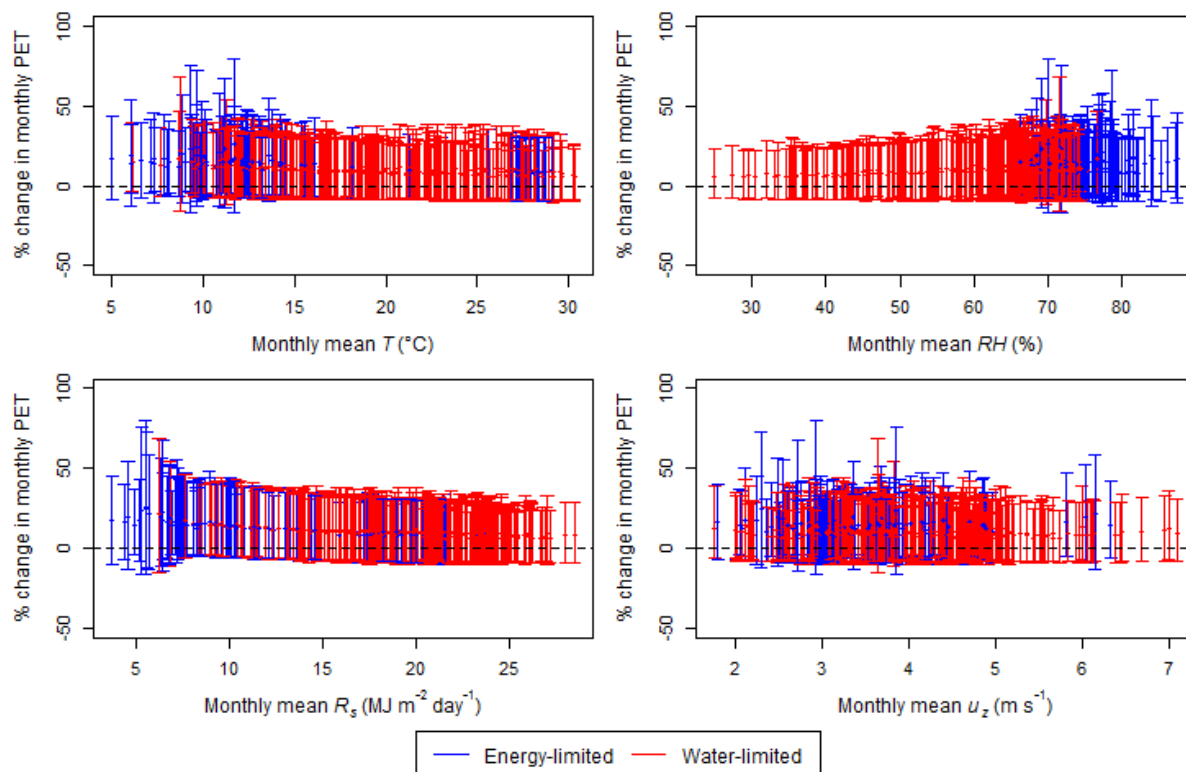
**Figure 2: Schematic of the method used in this study.**



721

722 **Figure 3:** Monthly PET responses from the Penman-Monteith model, plotted against the monthly baseline levels of (a)  
723 temperature, (b) relative humidity, (c) solar radiation and (d) wind speed at 30 study sites. Each interval represents  
724 the range of all PET responses to the full set of climate perturbations for a single month at a single location, with the  
725 mean represented by the point on the line. The classification of energy- and water-limited months are based on the  
726 corresponding monthly PET/P ratios.

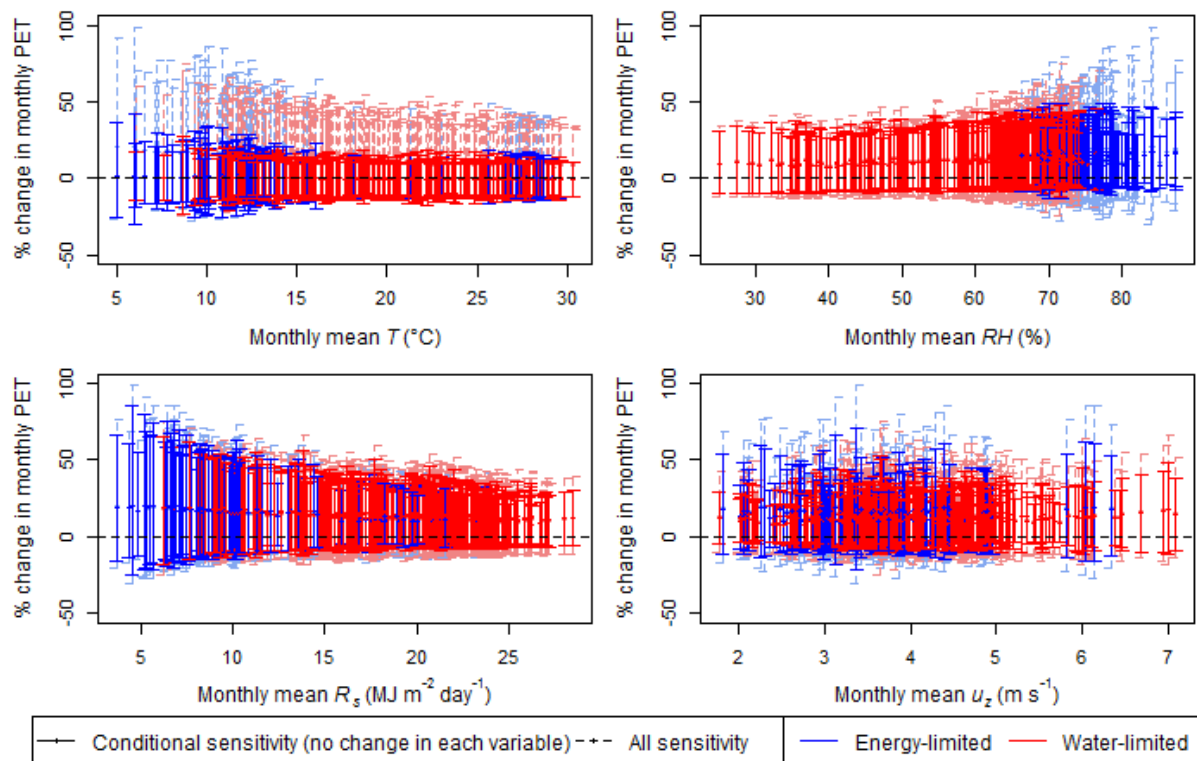
727



728

729 **Figure 4: Monthly PET responses from the Priestley-Taylor model, plotted against the monthly baseline levels of (a)**  
730 **temperature, (b) relative humidity, (c) solar radiation and (d) wind speed at 30 study sites. Each interval represents**  
731 **the range of all PET responses to the full set of climate perturbations for a single month at a single location, with the**  
732 **mean represented by the point on the line. The classification of energy- and water-limited months are based on the**  
733 **corresponding monthly PET/P ratios.**

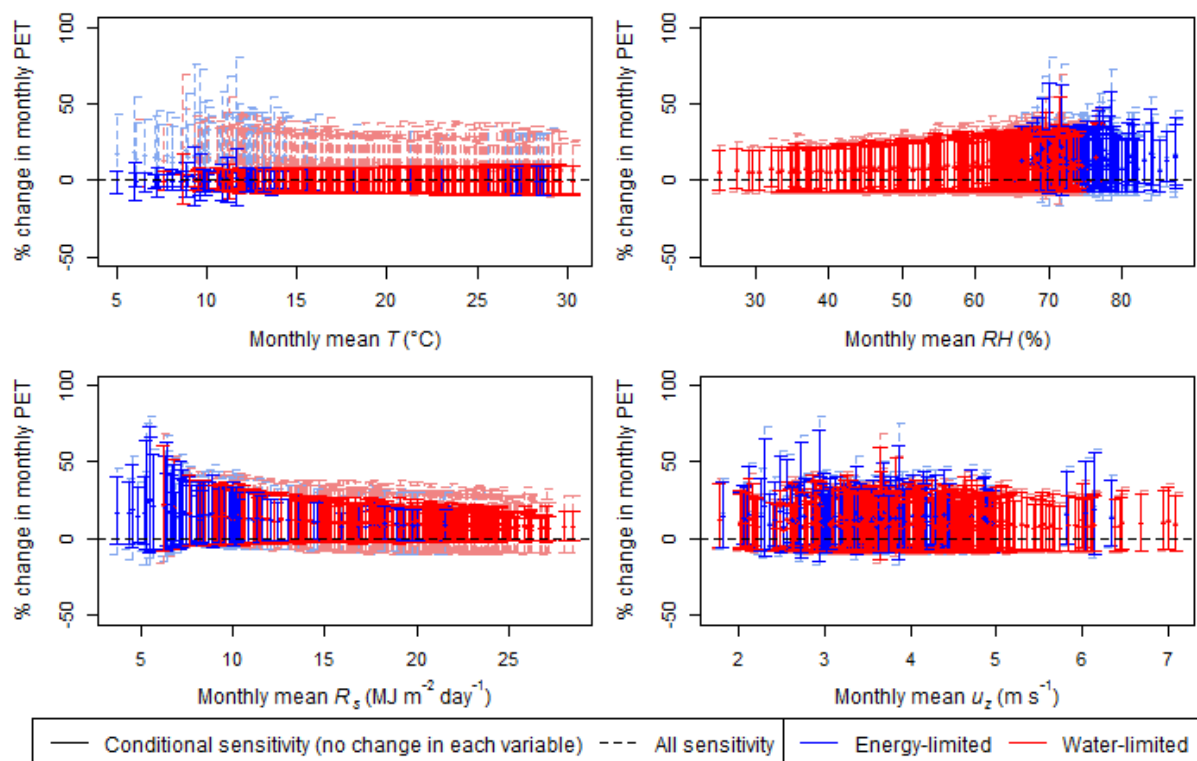
734



735

736 **Figure 5: Monthly PET responses from the Penman-Monteith model, plotted against the monthly baseline levels of (a)**  
 737 **temperature, (b) relative humidity, (c) solar radiation and (d) wind speed at 30 study sites. Each dashed (solid) line**  
 738 **represents the range of all PET responses to the full set of climate perturbations (conditioned on no-change in each**  
 739 **climate variable) for a single month at a single location. The corresponding means are represented by the points on**  
 740 **the lines. The classification of energy- and water-limited months are based on the corresponding monthly PET/P**  
 741 **ratios.**

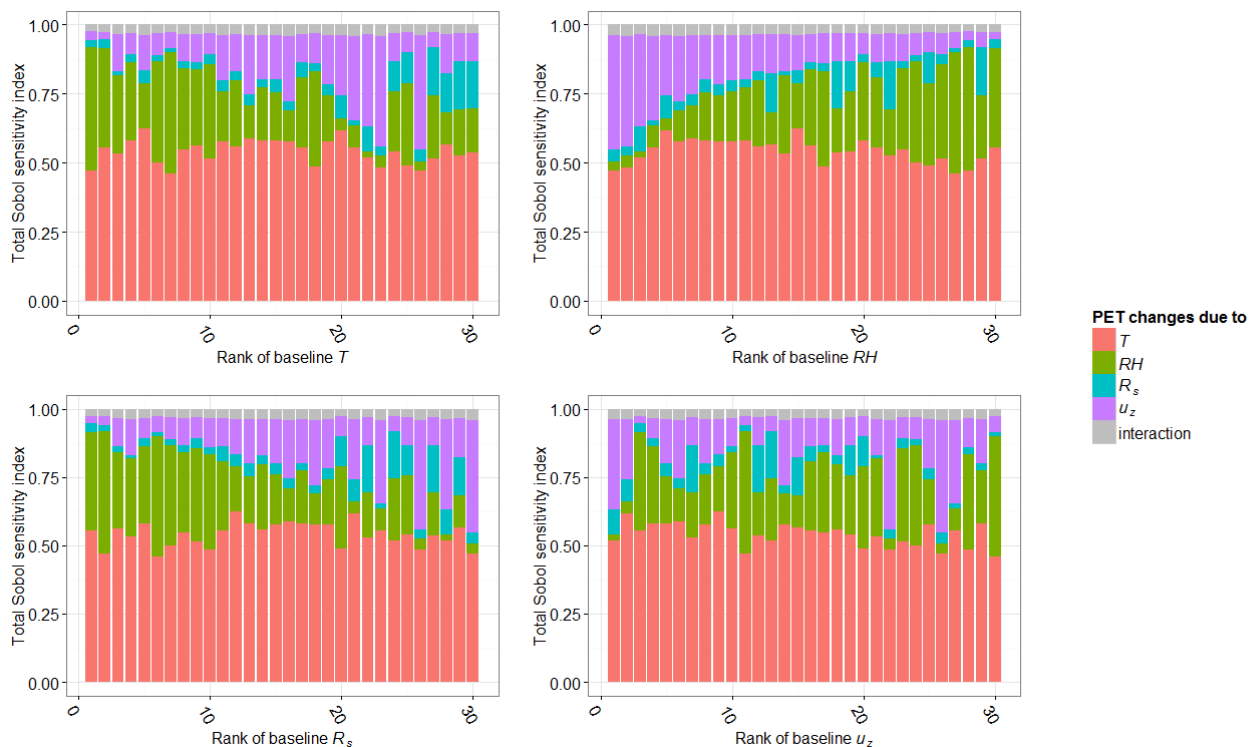
742



743

744 **Figure 6: Monthly PET responses from the Priestley-Taylor model, plotted against the monthly baseline levels of (a)**  
 745 **temperature, (b) relative humidity, (c) solar radiation and (d) wind speed at 30 study sites. Each dashed (solid) line**  
 746 **represents the range of all PET responses to the full set of climate perturbations (conditioned on no-change in each**  
 747 **climate variable) for a single month at a single location. The corresponding means are represented by the points on**  
 748 **the lines. The classification of energy- and water-limited months are based on the corresponding monthly PET/P**  
 749 **ratios.**

750



751  
752  
753  
754  
755  
756

**Figure 7: Sobol' first-order sensitivity indices of the Penman-Monteith model for changes in the four climate variables (colored) and their interaction effects (grey), plotted against the ranking of the average level of each climate variable at 30 study sites**

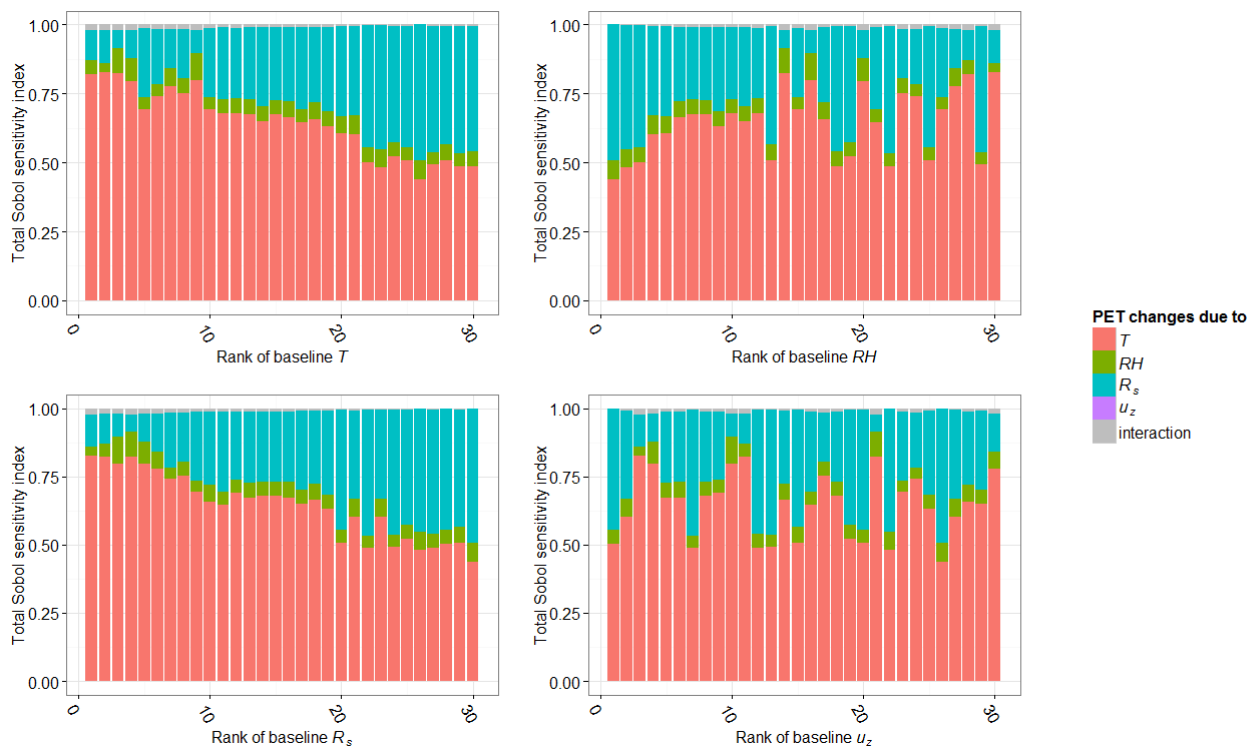


**Figure 8: Sobol' first-order sensitivity indices of the Priestley-Taylor model for changes in the four climate variables (colored) and their interaction effects (grey), plotted against the ranking of the average level of each climate variable at 30 study sites**

757  
 758  
 759  
 760  
 761  
 762



763 **Table 1: Names, locations and average climate conditions of the 30 weather stations over the study period (1995-**  
 764 **2004).**

No.	Study site name	Köppen class <sup>1</sup>	Lat (°S)	Long (°E)	Elev (m)	<i>T</i> (°C)	<i>RH</i> (%)	<i>R<sub>s</sub></i> (MJ m <sup>-2</sup> day <sup>-1</sup> )	<i>u<sub>z</sub></i> (m s <sup>-1</sup> )	Annual P (mm)	Annual PET (mm)	Annual PET/P
1	Broome airport	13	-17.95	122.2	7.4	26.37	65.15	21.55	3.684	865	2003	2.317
2	Perth	8	-31.93	116.0	15.4	18.54	61.72	18.95	4.519	721	1751	2.429
3	Albany	4	-34.94	117.8	68	15.08	73.59	15.20	4.382	752	1126	1.498
4	Giles	24	-25.03	128.3	598	22.70	38.40	20.29	4.380	394	2344	5.947
5	Darwin	35	-12.42	130.9	30.4	27.42	69.27	20.33	3.393	1976	1864	0.944
6	Gove	35	-12.27	136.8	51.6	26.29	75.93	19.45	3.500	1607	1660	1.033
7	Tennant Creek	13	-19.64	134.2	375.7	25.73	37.21	21.64	4.759	539	2634	4.886
8	Alice Springs	15	-23.80	133.9	546	21.18	44.53	20.79	2.352	331	1822	5.503
9	Woomera	24	-31.16	136.8	166.6	19.41	46.57	19.40	5.057	151	2153	14.24
10	Ceduna	11	-32.13	133.7	15.3	16.92	62.04	18.20	5.450	266	1723	6.478
11	Adelaide airport	12	-34.95	138.5	2	16.37	63.04	16.91	4.213	454	1410	3.107
12	Adelaide (kent town)	12	-34.92	138.6	48	16.95	61.20	16.88	3.161	569	1372	2.409
13	Loxton	12	-34.44	140.6	30.1	16.50	59.41	17.59	3.250	255	1490	5.847
14	Mount Gambier	4	-37.75	140.8	63	13.45	72.77	14.91	4.460	731	1116	1.526
15	Weipa	41	-12.68	141.9	18	26.87	72.21	19.31	3.271	2154	1782	0.827
16	Cairns	36	-16.87	145.7	3	24.80	73.00	18.98	4.352	1985	1678	0.845
17	Townsville	35	-19.25	146.8	4.3	24.53	69.45	20.27	4.304	1099	1802	1.641
18	Cobar	15	-31.48	145.8	260	19.08	50.64	19.05	2.458	398	1565	3.936
19	Williamstown	9	-32.79	151.8	9	17.84	70.57	16.07	3.927	1145	1309	1.143
20	Sydney	9	-33.94	151.2	6	18.19	67.69	15.97	5.311	1017	1393	1.369
21	Canberra	6	-35.30	149.2	578.4	13.36	65.82	16.86	3.302	590	1226	2.078
22	Wagga Wagga	9	-35.16	147.5	212	15.77	61.78	17.48	3.288	552	1436	2.602
23	Mildura	12	-34.24	142.1	50	17.11	55.62	18.24	3.604	246	1645	6.681
24	East sale	6	-38.12	147.1	4.6	13.77	72.32	14.92	4.062	529	1093	2.067
25	Scottsdale	3	-41.17	147.5	197.5	13.19	70.55	14.23	2.921	931	912	0.980
26	Bicheno	3	-41.87	148.3	11	14.69	66.68	13.69	3.319	690	966	1.401
27	Lake Leake	3	-42.01	147.8	575	9.96	75.40	13.44	3.358	732	774	1.056
28	Hobart	3	-42.83	147.5	4	12.77	65.67	14.04	4.367	483	1097	2.273
29	Strathgordon village	3	-42.77	146.0	322	10.70	77.95	11.65	2.473	2626	699	0.266





---

30	Flinders Island	3	-40.09	148.0	9	13.54	73.59	14.34	6.399	654	1064	1.626
----	--------------------	---	--------	-------	---	-------	-------	-------	-------	-----	------	-------

---

765 **Note:**

766 <sup>1</sup>The Köppen classes are presented with their corresponding identifiers from Stern et al. (2000), as: 3. Temperate - no  
767 dry season (mild summer); 4. Temperate - distinctly dry (and warm) summer; 6. Temperate - no dry season (warm  
768 summer); 8. Temperate - moderately dry winter (hot summer); 9. Temperate - no dry season (hot summer); 11.  
769 Grassland - warm (summer drought); 12. Grassland - warm (persistently dry); 13. Grassland - hot (winter drought);  
770 15. Grassland - hot (persistently dry); 24. Desert - hot (persistently dry); 35. Tropical - savanna; 36. Tropical -  
771 rainforest (monsoonal); 41 Equatorial - savanna.

772 <sup>2</sup> $T$  = temperature,  $RH$  = relative humidity,  $R_s$  = incoming solar radiation,  $u_z$  = wind speed,  $P$  = rainfall, PET = potential  
773 evapotranspiration calculated using the Penman-Monteith model.

774



775 **Table 2: Plausible perturbation bounds for each climate variable relative to their current levels.**

Climate variable	Perturbation range
$T$	0 to +8 °C
$RH$	-10 % to +10 %
$R_s$	-10 % to +10 %
$u_z$	-20 % to +20 %

776 **Note:**  $T$  = daily temperature,  $RH$  = daily relative humidity,  $R_s$  = daily incoming solar radiation,  $u_z$  = daily wind  
777 speed.

778



779 **Table 3: Annual average PET sensitivity to the full set of climate perturbations (as % changes to baseline PET) from**  
 780 **the Penman-Monteith and Priestley-Taylor models at the 30 study sites relative to the 1995-2004 baseline. The**  
 781 **maximum and minimum sensitivity values from each model are shaded in grey.**

No.	Study site name	Penman-Monteith			Priestley-Taylor		
		Min.	Max.	Avg.	Min.	Max.	Avg.
1	Broome airport	-12.33	39.10	11.16	-9.61	33.75	9.59
2	Perth	-13.20	46.67	13.52	-7.98	34.17	10.62
3	Albany	-15.04	54.67	15.21	-7.28	35.49	11.63
4	Giles	-12.30	37.57	10.68	-7.73	25.83	7.27
5	Darwin	-12.73	39.10	10.92	-9.82	33.84	9.50
6	Gove	-13.10	41.34	11.53	-9.74	33.67	9.61
7	Tennant Creek	-12.28	36.45	10.21	-8.35	26.31	7.09
8	Alice Springs	-10.88	34.00	9.80	-8.00	27.41	7.92
9	Woomera	-12.84	43.48	12.73	-7.48	30.35	9.18
10	Ceduna	-13.97	49.61	14.39	-7.62	33.82	10.67
11	Adelaide airport	-14.47	49.80	14.17	-7.22	34.55	11.09
12	Adelaide (kent town)	-13.10	45.43	13.17	-7.15	33.70	10.78
13	Loxton	-12.55	44.05	12.96	-7.18	33.34	10.67
14	Mount Gambier	-15.33	57.97	16.00	-6.58	35.54	12.02
15	Weipa	-12.42	39.06	10.95	-9.66	32.98	9.36
16	Cairns	-14.80	44.74	12.08	-9.42	33.84	9.73
17	Townsville	-13.77	43.21	12.10	-9.43	34.26	9.90
18	Cobar	-10.62	37.49	11.36	-7.64	31.19	9.49
19	Williamstown	-13.64	47.99	13.68	-7.66	34.11	10.76
20	Sydney	-16.24	53.71	14.46	-7.61	35.24	10.98
21	Canberra	-12.41	46.17	13.85	-6.95	33.24	10.92
22	Wagga Wagga	-13.00	46.34	13.43	-7.09	33.27	10.74
23	Mildura	-12.61	44.50	13.05	-7.24	32.75	10.38
24	East sale	-14.43	53.82	15.34	-6.51	36.32	12.19
25	Scottsdale	-13.64	51.53	15.02	-5.42	40.00	13.47
26	Bicheno	-14.81	52.11	14.87	-4.91	46.38	15.68
27	Lake Leake	-16.06	60.36	16.45	-5.11	36.03	12.84
28	Hobart	-15.97	56.29	15.78	-4.57	50.36	17.77
29	Strathgordon village	-13.08	52.11	15.29	-4.66	33.83	12.35
30	Flinders Island	-18.05	64.07	17.15	-6.19	38.66	13.02
<b>Average</b>		<b>-13.66</b>	<b>47.09</b>	<b>13.38</b>	<b>-7.39</b>	<b>34.47</b>	<b>10.91</b>

782